Published OnlineFirst July 5, 2017; DOI: 10.1158/1078-0432.CCR-17-0802

Biology of Human Tumors

Clinical Cancer Research

Sequential Tracking of PD-L1 Expression and RAD50 Induction in Circulating Tumor and Stromal Cells of Lung Cancer Patients Undergoing Radiotherapy

Daniel L. Adams[1], Diane K. Adams[2], Jianzhong He[3], Neda Kalhor[3], Ming Zhang[4], Ting Xu[3], Hui Gao[3], James M. Reuben[3], Yawei Qiao[3], Ritsuko Komaki[3], Zhongxing Liao[3], Martin J. Edelman[5], Cha-Mei Tang[6], and Steven H. Lin[3]

Abstract

Purpose: Evidence suggests that PD-L1 can be induced with radiotherapy and may be an immune escape mechanism in cancer. Monitoring this response is limited, as repetitive biopsies during therapy are impractical, dangerous, and miss tumor stromal cells. Monitoring PD-L1 expression in both circulating tumor cells (CTCs) and circulating stromal cells (CStCs) in blood-based biopsies might be a practical alternative for sequential, noninvasive assessment of changes in tumor and stromal cells.

Experimental Design: Peripheral blood was collected before and after radiotherapy from 41 patients with lung cancer, as were primary biopsies. We evaluated the expression of PD-L1 and formation of RAD50 foci in CTCs and a CStC subtype, cancer-associated macrophage-like cells (CAMLs), in response to DNA damage caused by radiotherapy at the tumor site.

Results: Only 24% of primary biopsies had sufficient tissue for PD-L1 testing, tested with IHC clones 22c3 and 28-8. A CTC or CAML was detectable in 93% and 100% of samples, prior to and after radiotherapy, respectively. RAD50 foci significantly increased in CTCs (>7×, $P < 0.001$) and CAMLs (>10×, $P = 0.001$) after radiotherapy, confirming their origin from the radiated site. PD-L1 expression increased overall, 1.6× in CTCs ($P = 0.021$) and 1.8× in CAMLs ($P = 0.004$): however, individual patient PD-L1 expression varied, consistently low/negative (51%), consistently high (17%), or induced (31%).

Conclusions: These data suggest that RAD50 foci formation in CTCs and CAMLs may be used to track cells subjected to radiation occurring at primary tumors, and following PD-L1 expression in circulating cells may be used as a surrogate for tracking adaptive changes in immunotherapeutic targets. *Clin Cancer Res; 23(19); 5948–58. ©2017 AACR.*

Introduction

Liquid biopsies provide real-time sequential tracking of circulating tumor cells (CTC) found in the peripheral blood, acting as a substitute to follow-up tissue biopsies (1–4). Assessing circulating tumor cells (CTC) in the peripheral blood has the power to interrogate heterogeneous populations of CTCs, including CTC subtypes undergoing epithelial-to-mesenchymal transition (EMTCTC; refs. 2, 3, 5–9) and the prognostically relevant pathologically definable CTCs (PDCTC; refs. 6–10). However, the utilization of cancer-associated circulating stromal cells (CStCs) has not been well studied in liquid biopsies. Recently, we have identified a prevalent CStC subtype, cancer-associated macrophage-like cells (CAMLs), using a nonaffinity microfiltration–based method that captures both CTCs and CAMLs and allows for parallel analysis of these cancer-specific circulating cell subtypes (1, 6–16). CAMLs are recently defined circulating myeloid-derived stromal cells, found in all the stages of invasive malignancy and in various solid malignancies [e.g., breast, prostate, non–small cell lung carcinoma (NSCLC), and pancreatic; refs. 11, 13, 14, 17]. CAMLs are defined by their CD45/CD14 positivity and giant size phenotype (11, 13, 14, 17). Although CAMLs appear to be cancer specific and disseminate from the organ sites of malignancy, it remains unknown whether they actually reside at the primary tumor site or whether they possess clinical utility.

Cells originating from tumors receiving site-directed radiation are marked by ionizing radiation–induced DNA damage, including tumor and stromal cells (18–24). Thus, we expect that circulating cells that originate at the tumor site during radiotherapy should have evidence of DNA damage, such as ionizing radiation–induced foci (IRIF), which can be visualized with RAD50 (18–24). RAD50 is a protein that complexes with the proteins NBS1 and MRE11 and is crucial in the DNA double-strand repair process following treatment with radiation and/or chemical

[1]Creatv MicroTech, Inc., Monmouth Junction, New Jersey. [2]Rutgers, the State University of New Jersey, New Brunswick, New Jersey. [3]MD Anderson Cancer Center, Houston, Texas. [4]Hebei General Hospital, Shijiazhuang, China. [5]Fox Chase Cancer Center, Philadelphia, Pennsylvania. [6]Creatv MicroTech, Inc., Potomac, Maryland.

Note: Supplementary data for this article are available at Clinical Cancer Research Online (http://clincancerres.aacrjournals.org/).

Corresponding Authors: Dan L. Adams, Creatv Microtech, Inc., 1 Deer Park Dr #L4, Monmouth Junction, NJ 08852. Phone: 301-861-4924; Fax: 301-983-6264; E-mail: dan@creatvmicrotech.com; and Steven H. Lin, Department of Radiation Oncology, MD Anderson Cancer Center, Houston, TX 77030. Phone: 713-563-8490; Fax: 713-563-2300; E-mail: shlin@mdanderson.org

doi: 10.1158/1078-0432.CCR-17-0802

Published OnlineFirst July 5, 2017; DOI: 10.1158/1078-0432.CCR-17-0802

Translational Relevance

Classically, cancer drugs focus on targets identified in tumor biopsies using IHC analysis. However, newer immune-modulating drug targets, that is, PD-L1, are expressed on numerous cell types, including tumor cells and stromal cells (e.g., macrophages), which are not always observable in biopsies. Complicating the ability to profile immune modulation is that stroma–tumor interaction is dynamic, changing over time, with treatment, and difficult to track using a single biopsy. We hypothesized that blood-based biopsies might be utilized in tracking dynamic alterations of tumor and stromal biomarkers in real time by noninvasive sequential approaches. We prospectively quantified the biological changes of PD-L1 expression and RAD50 foci before and after radiotherapy induction in circulating tumor cells and circulating stromal cells. Our findings indicate that circulating cells might be used to systematically quantify biological changes in cells emanating from the primary tumor as they relate to immune modulation.

agents. In normal mammalian cells, RAD50 is distributed throughout both the cytoplasm and the nucleus. Following double-stranded breaks in DNA, the RAD50/NBS/MRE11 complex rapidly translocates to the sites of the breakage, forming aggregated nuclear foci until the break is repaired, for example, IRIF (18, 20, 23, 25). Thus, RAD50 can be used as a specific identifier of cells that have been exposed to high levels of radiation, acting as a biological tag of cells from patients that have been directly exposed to radiation targeted to a tumor mass (18–24, 26–28).

PD-L1/PD-1 immune blockade drugs (e.g., nivolumab and pembrolizumab) are potent immune checkpoint inhibitors that have been shown to dramatically shrink and stabilize tumors in approximately 20% of patients with NSCLCs (29–40). These types of immunotargeted therapeutics specifically alter a patient's stromal interactions by activating the host's immune cell response against the presence of tumor cells (29–36, 41, 42). A number of validated IHC assays have recently been developed to assess PD-L1 expression within tumor sample biopsies. In IHC biopsy testing, it is well known that although high expressing PD-L1 tumors respond better to anti-PD-L1/PD-1 therapies, a significant number (~20%) of patients with low or no PD-L1 in their tumors will also respond (29–34, 36–40, 42). Thus, there are suggestions that PD-L1 may be induced by therapies, such as targeted agents, cytotoxic chemotherapy, or radiotherapy, which may act as an immunologic escape response in tumors (29–34, 36–40, 42). We hypothesize that a subset of patients with low or no PD-L1 expression in pretreatment tumors will be induced to express PD-L1 during therapy and these tumors will respond to immune checkpoint inhibitors. As repeat biopsies are impractical during the course of therapy, especially in patients with nonmetastatic lung cancer, assessing PD-L1 expression on CTCs and CAMLs using blood-based biopsies (BBBs) may allow serial assessment of the status of PD-L1 expression during therapy (29–34, 36–40, 42).

For this study, we prospectively tracked 41 patients with lung cancer, drawing blood samples at a pretreatment baseline time point (T0) prior to the start of radiotherapy or chemoradiation therapy and a follow-up T1 blood sample after the start of radiotherapy (i.e., ~14–21 days after radiotherapy).We compared the expression of PD-L1 on PDCTCs, EMTCTCs, and CAMLs with the available primary tumor biopsies. However, proper comparison of PD-L1 in tissue biopsies was not possible as tissue was limited in lung cancer biopsies. To determine whether the circulating cells originated from the irradiated tumor site, we also assayed for RAD50 foci formation, a marker of DNA double-stranded break repair that occurs after radiation damage. Our data suggest that PD-L1 and the formation of RAD50 foci can be sequentially tracked in CAMLs and CTCs. Our data suggest that CAMLs and CTCs isolated from blood originate from the primary lung tumors, and an upregulation of PD-L1 can be identified in these circulating cells.

Materials and Methods

Blood sample collection

Forty-one patients with stage I–IV lung cancer were included in this prospective pilot study (Supplementary Table S1). Anonymized peripheral blood samples were collected after written informed consent and according to the local Institutional Review Board (IRB) approval. Patients were recruited from July 2013 to May 2014 prior to starting radiotherapy for primary lung cancer. Four patients received stereotactic body radiotherapy (SBRT) for stage I disease, and 37 patients received chemoradiation for stage II–IV disease with proton therapy ($n = 16$) or intensity-modulated radiotherapy ($n = 21$). Anonymized blood samples (7.5 mL) were drawn and processed on site at the MD Anderson Cancer Center (MDA, Houston, TX). Slides were anonymized, then shipped and analyzed at Creatv MicroTech, Inc.'s clinical core laboratory. Anonymized biopsy samples from primary tumors were processed at MDA according to manufacturer's protocols (DAKO). Results from institutions were not shared or communicated until the completion of the study. In addition, anonymized healthy control blood samples ($n = 10$) were procured with written informed consent and IRB approval by Western IRB. Volunteer donor blood was procured on a voluntarily basis at a collection center with no selection process other than standard exclusion criteria.

CellSieve low-flow microfiltration procedure

Blood samples (7.5 mL) collected in CellSave preservative tubes were processed with a CellSieve Microfiltration Assay using a low-pressure vacuum system (1, 12). CellSieve Microfiltration Assay isolates circulating cells based on size exclusion, >7 μm. A trained cytologist identified PDCTCs, EMTCTCs, and CAMLs based on morphologic features and the phenotypic expression of CD45, EpCAM, cytokeratins 8, 18, 19, and DAPI (Fig. 1; Supplementary Fig. S1; refs. 1, 6, 12) using preestablished cytologic features described previously (6, 11, 14). An Olympus BX54WI Fluorescent microscope with Carl Zeiss AxioCam and Zen2011 Blue (Carl Zeiss) was used for all imaging.

Enumerating PDCTC/EMTCTC subtypes and CAMLs

We have previously described the defining characteristics of the two most common CTC subtypes found in cancer patients (PDCTCs and EMTCTCs), and for CAML identification (1, 6, 10–14). For this study, only intact PDCTCs, EMTCTCs, and CAMLs were characterized (Fig. 2; Supplementary Fig. S1; refs. 1, 6, 10–14). PDCTCs are CD45 negative, with filamentous

Published OnlineFirst July 5, 2017; DOI: 10.1158/1078-0432.CCR-17-0802

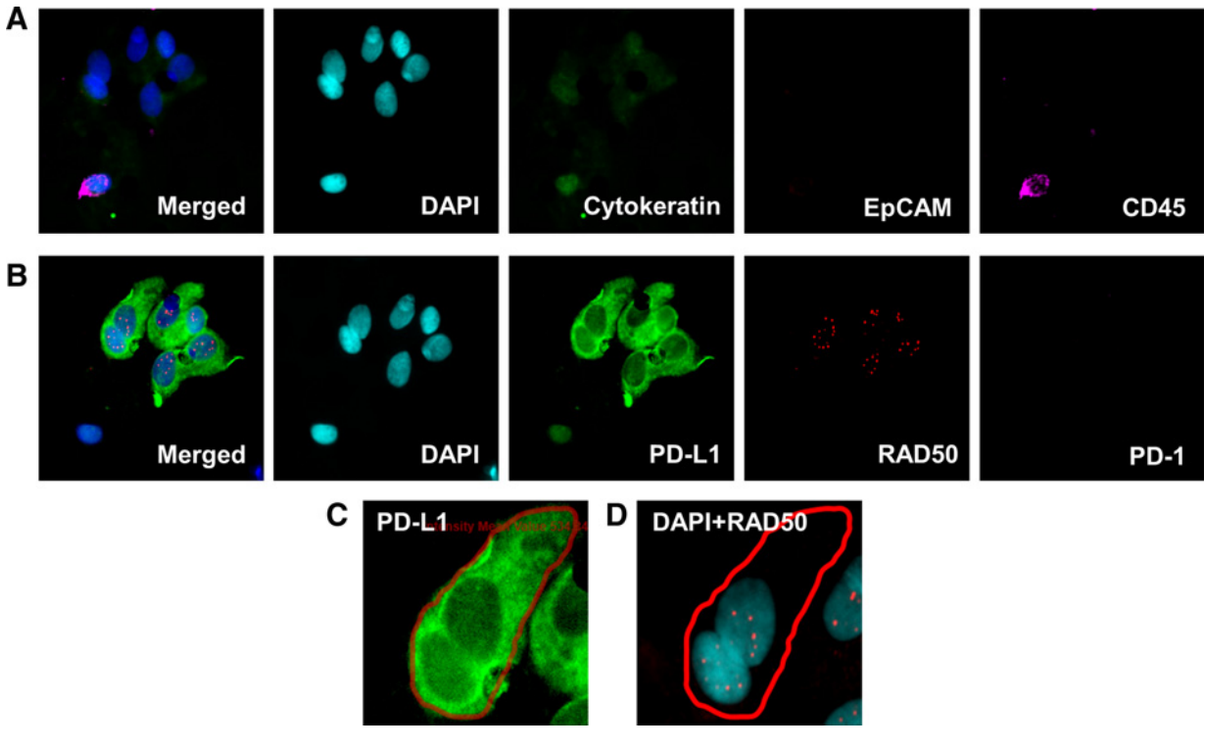

Figure 1.

A BBB identifies and subtypes circulating cells by DAPI, cytokeratin, EpCAM, and CD45; then, the QUAS-R fluorescence quenching technique is used to restain cells with RAD50 and PD-L1. **A,** An example of a EMTCTC cluster of cells, weakly positive for cytokeratin, negative for EpCAM, and negative for CD45. Box scale, 90 μm. **B,** The sample is quenched by QUAS-R where the fluors are quenched without harming the protein epitopes (13). The samples are then restained with PD-L1, RAD50, and PD-1. Box scale, 90 μm. **C,** PD-L1 is measured by tracing the cell in Zen software, which calculated the average intensity of each cell or cell cluster. Box scale, 35 μm. **D,** RAD50 foci (red) are enumerated in each nucleus (cyan). Box scale, 35 μm.

cytokeratin positivity and DAPI-positive nuclei with malignant pathologic criteria, classified as the CellSearch subtype of CTC (1, 6, 10–14). EMTCTCs are CD45 negative with a diffuse cytokeratin signal and a DAPI-positive nucleus with abnormal criteria, as defined previously (1, 6–9, 12, 13). CAMLs are described as enlarged (>30 μm), multinuclear cells with diffuse cytoplasmic cytokeratin staining, and/or $CD45^{+}/CD14^{+}$ (6, 11, 14, 17, 22, 43). All three cell types were identified and imaged by a trained CTC cytologist and confirmed by a pathologist. Apoptotic CTCs and CTCs that could not be cytologically classified as previously described were not included in this study. After identification, cells were imaged, and the x–y axis of each cell was marked for future analysis. Samples were archived at 4°C for 1 to 3 years.

QUAS-R quenching and restaining for PD-L1 and RAD50

After initial identification and quantification of PDCTCs, EMTCTCs, and CAMLs, fluorescence was quenched, and samples were restained with RAD50-DyLight 550 (Pierce Thermo), PD-L1-AlexaFluor 488 (R&D systems), and DAPI nuclear stain (Fig. 1). The QUAS-R (Quench, Underivatize, Amine-Strip, and Restain) technique was used as described previously (13). Briefly, after samples were imaged and marked, filters were subjected to a sequential chemical treatment of quenching solution, Tris, and wash steps. After chemical quenching, filters were washed with PBS, incubated with 1× PBS/20%FBS, and then incubated with antibodies against RAD50-AlexaFluor550 and PD-L1-AlexaFluor 488 for 1 hour at room temperature. After antibody incubation, filters are washed in 1× PBST and slide mounted with Fluoromount-G/DAPI (SouthernBiotech). Samples were oriented along the x/y axis, and previously imaged cells were relocated using a Zen2011 Blue (Carl Zeiss) mark and find software. A Zen2011 Blue (Carl Zeiss) was used to process the images.

Quantifying PD-L1 in primary tumor biopsies

PD-L1 expression from all available primary tumor biopsies were analyzed using both DAKO pharmdx clone 22c3 and DAKO pharmdx clone 28-8 according to the manufacturer's guidelines (Fig. 3). Eight patients from the study had sufficient and available archived tumor samples to screen both clones, and one sample had sufficient archived tumor for a single IHC test against clone 22c3. Both clones were stained according to standard operating procedures described previously (29–31, 38).

Quantifying RAD50 and PD-L1 in circulating cells

RAD50 loci formation was determined by enumerating the nuclear localized RAD50 loci in each cell (Supplementary Fig. S2; Fig. 1; ref. 23). PD-L1 pixel intensity of each cell was measured by the ZenBlue software by using the area of the entire cell. The average pixel intensity of each cell was subtracted from the average pixel intensity of the local background for each image (Fig. 1C). The average pixel intensity of the cells was quartiled into four IHC groups: 0, negative (pixel average, 0–150); 1, low (pixel

Published OnlineFirst July 5, 2017; DOI: 10.1158/1078-0432.CCR-17-0802

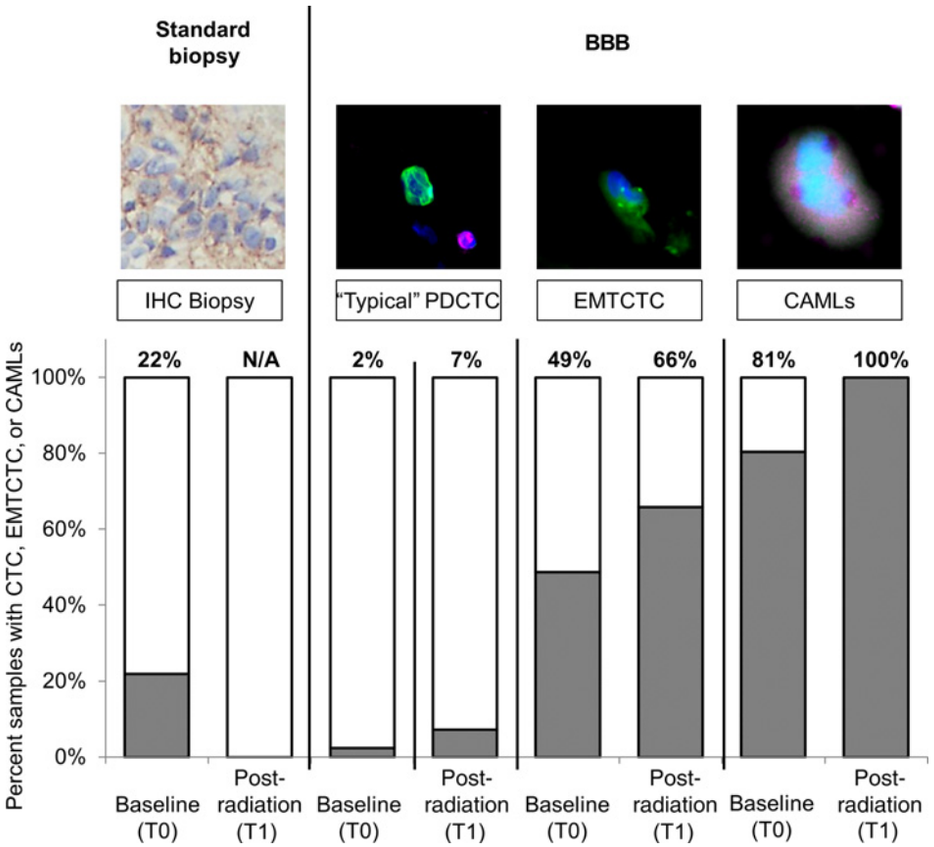

Figure 2.
Percentage of samples with cells that could be used to quantify PD-L1 at baseline (T0) and postinduction of radiotherapy (T1); BBBs include two subtypes of circulating tumor cells and circulating stromal cells. Standard biopsies only have the initial baseline time points, and only 22% of those samples had sufficient amount of tumor for analysis by PD-L1. Brown stain is PD-L1/blue is hematoxylin. A BBB identified EMT tumor cells in 49% of baseline samples and in 66% of posttherapy samples. Furthermore, CAMLs were available in 81% of baseline samples and in 100% of follow-up samples. Blue, DAPI; green, cytokeratin; purple, CD45; boxes, 65 μm.

average, 151–300); 2, medium (pixel average, 301–750); and 3, high (pixel average, 751+; Supplementary Fig. S2). IHC range thresholds of PD-L1 intensity for IHC scoring were determined as: 150 pixel intensity was the standard deviation of the localized background signal, 300 pixel intensity was twice the SD of the localized background, and 750 was twice the intensity of the localized background (Supplementary Fig. S2).

Statistical analysis

Analyses were done in MATLAB R2013A using the counts from all subtypes and the known patient populations. For progression-free survival analysis, the time to progression was defined as the interval between when T0 blood sample was obtained and date of progression; all patients remained on study through 24-month endpoint, that is, no patients were censored. Significance of the average changes in RAD50 foci formation and PD-L1 expression were determined by a Student *t* test. A Pearson coefficient was used to determine the correlation between RAD50 foci and PD-L1 expression for individual measurements. Significance of Kaplan–Meier plots was determined by log-rank analysis.

Results

PDCTCs, EMTCTCs, and CAMLs in patients with lung cancer

Prior reports indicate that the CTC subpopulation in patients with NSCLC using the CellSearch platform is typically found in only 0% to 5% of nonmetastatic cases. In contrast, the EMTCTC population is typically found in approximately 80% of nonmetastatic patient populations, while CAMLs have not been extensively evaluated in NSCLC (3–6, 8, 15, 17, 43–45). In the first baseline blood sample taken prior to the start of radiotherapy (T0), we were able to identify at least one cytokeratin-positive cell (i.e., PDCTC, EMTCTC, or CAML; Figs. 1, and 2) in 35 of the 41 samples (85%). In a small group of 10 healthy controls, no CAMLs, CTCs, nor EMTCTCs were found. This is in agreement with our previous studies (1, 6, 10–14). Patients then had a second follow-up sample (T1) taken 2 to 3 weeks after radiotherapy initiation or after the last fraction for SBRT patients. For T1, there was at least one cytokeratin-positive cell (i.e., PDCTC, EMTCTC, or CAML) found in all 41 samples (100%). Specifically, EMTCTCs were found in 49% of T0 samples and in 66% of T1 samples. CAMLs were found in 81% of T0 samples and in 100% of T1 samples (Fig. 2). PDCTCs were found in only one sample at T0 (2%) and in only three samples at T1 (7%; Fig. 2). Being that PDCTCs have been shown to be the same CTC population of cells isolated by the CellSearch® CTC System, these numbers are on par with previous reports (7–9, 15). The CellSearch system isolates CTCs in patients with NSCLC ranging from approximately 0% to 5% positivity in stage III NSCLC and 21% to 32% in stage IV (7–9, 15). As 35 of the patients were staged as I–III, 2% to 7% is within the range of the classical CTC population (Supplementary Table S1; refs. 7–9, 15). The low incidence of the classical PDCTC population (Fig. 2) is in contrast to EMTCTC and CAMLs, which are present in 85% (T0) and 100% (T1) of the samples. Although it has been postulated that EMTCTCs alone may provide some increased sensitivity for liquid biopsies in NSCLC (7–9, 16), these results suggest that the combination

Published OnlineFirst July 5, 2017; DOI: 10.1158/1078-0432.CCR-17-0802

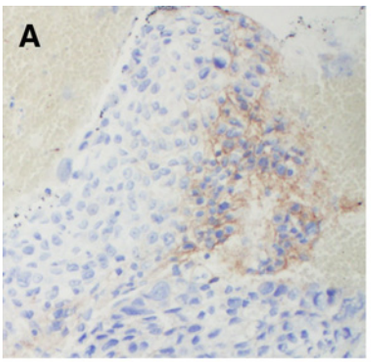

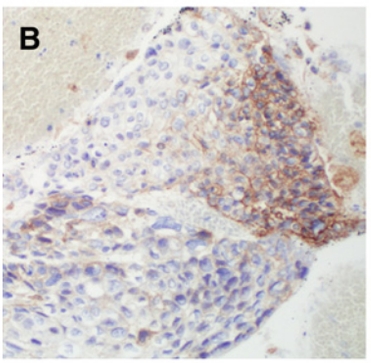

C

ID#	T0 (%/SI)	22c3 (%/SI)	28-8 (%/SI)
1	17/2	0	0
2	100/3	0	0
3	33/1	0	0
4	100/1	0	0
5	33/1	0	N/A
6	N/A	0	0
7	50/2	0	0
8	33/2	10/1+	20/2+
9	80/3	40/2+	80/3+
10	25/0	N/A	N/A
11	100/0	N/A	N/A
12	100/0	N/A	N/A
13	100/0	N/A	N/A
14	51/1	N/A	N/A
15	100/1	N/A	N/A
16	50/1	N/A	N/A
17	13/1	N/A	N/A
18	100/1	N/A	N/A
19	50/1	N/A	N/A
20	100/1	N/A	N/A
21	86/1	N/A	N/A
22	75/1	N/A	N/A
23	50/1	N/A	N/A
24	100/1	N/A	N/A
25	100/1	N/A	N/A
26	50/1	N/A	N/A
27	75/2	N/A	N/A
28	20/2	N/A	N/A
29	100/2	N/A	N/A
30	72/2	N/A	N/A
31	100/2	N/A	N/A
32	100/2	N/A	N/A
33	4/3	N/A	N/A
34	13/3	N/A	N/A
35	100/3	N/A	N/A
36	100/0	N/A	N/A
37	N/A	N/A	N/A
38	N/A	N/A	N/A
39	N/A	N/A	N/A
40	N/A	N/A	N/A
41	N/A	N/A	N/A

Figure 3.
Testing and comparing the clinically approved IHC PD-L1 clones from DAKO and the BBB PD-L1 clone. **A,** Clone 22c3 from patient ID# 8 sample, which scored 1+ in 10% of the tumor. **B,** Clone 28-8 from patient ID# 8 parallel sample, which scored 2+ in 20% of the tumor. **C,** A PD-L1 clone optimized for BBBs was used to determine the number of cells positive for PD-L1 and the intensity of each cell found on the CellSieve microfilters. SI, pixel intensity quartile; %, percent of cells positive for the maximum pixel intensity quartile; N/A, no available sample to test.

of both EMTCTCs and CAMLs provides improved sensitivity analyzing tumor-derived cells for blood-based diagnosis.

RAD50 as a biological tracker of irradiated cells

Although CTCs and CAMLs have been described as disseminating into peripheral blood from the site of a primary tumor, studies have yet to confirm the exact location that these cells reside in prior to entry into circulation. The primary reason for this unknown origin is because labeling tumor/stromal cells in patients and tracking their dissemination is difficult, as such experiments pose a danger to patients. Although RAD50 foci within IRIF formations in mammalian cells have been shown as a biological tracker of direct radiation exposure to cells, this has never been evaluated in circulating tumor or stromal cells in patients undergoing radiation. In nonirradiated lung cancer patients at T0 baseline, RAD50 foci in EMTCTCs cells ranged from 0 to 4 per nuclei with an average of 0.59 ± 0.97 foci, and in CAMLs, the foci number ranged from 0 to 5 with an average of 0.38 ± 1.07 (Fig. 4; Supplementary Fig. S3). The presence of some RAD50 foci in cells is not surprising as RAD50 foci is a normal biological repair mechanism that is typically identified in a small number of untreated cells (21, 23, 24). After patients were

Published OnlineFirst July 5, 2017; DOI: 10.1158/1078-0432.CCR-17-0802

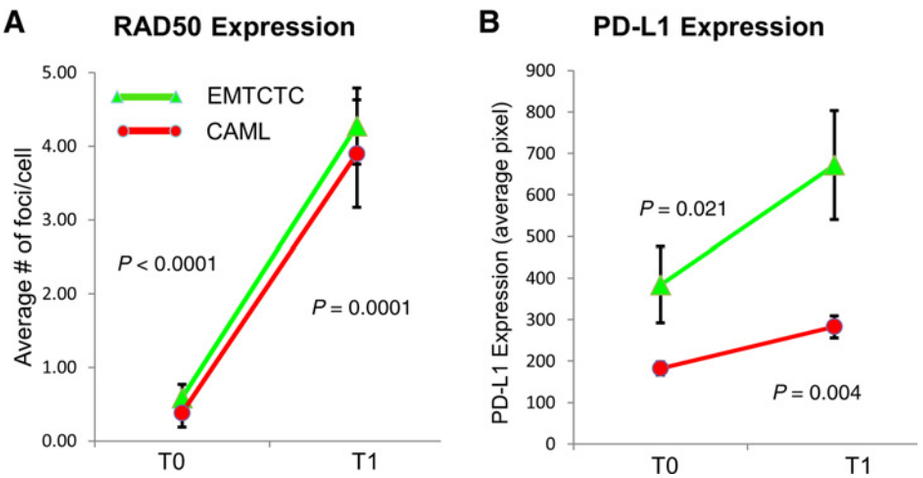

Figure 4.
Dynamic changes in the formation of RAD50 loci within the nucleus and the upregulation of PD-L1 on cells analyzed in both circulating tumor cells and stromal cells throughout treatment using a BBB approach. **A,** Formation of RAD50 foci can be accurately enumerated, and a clear increase in RAD50 loci was observed after the induction of radiotherapy (Supplementary Fig. S5). This suggests that both EMTCTC and CAMLs are originating from the site of radiation. **B,** PD-L1 can be evaluated in both EMTCTCs and CAMLs originating from the primary tumor site. Error bars, SE.

exposed to tumor-directed radiotherapy at T1, RAD50 foci in EMTCTCs significantly increased to 0 to 9 per nuclei with an average of 4.27 ± 2.63, and in CAMLs, the number increased to 0 to 20 with an average of 3.9 ± 3.93 per nuclei (Fig. 4). This increase was observed in all patients with detectable cells at both T0 and T1 time points ($n = 35$) and was rarely found in any background of normal $CD45^+$ leukocytes (Fig. 1B). Thus, RAD50 in both EMTCTCs and CAMLs increased from an average of 0.48 at T0 to an average of 4.05 ($P < 0.0001$) at T1 (Fig. 4). These results suggest that RAD50 may be used to label and track the irradiated cells that originate at tumor sites and, thus, can be used to track tumor dynamics.

Dynamic expression of PD-L1 in circulating cells

There have been suggestions that PD-L1 may be induced in tumors by various cytotoxic therapies, including radiation (29–34, 36–40, 42). To determine whether this could be seen using BBB, we evaluated PD-L1 staining at the T0 and T1 time points. A normalized comparative scoring system was developed in a similar manner to the classical 0 to 3 IHC tissue biopsy scoring (Fig. 5; Supplementary Fig. S2). After staining and imaging, PD-L1 expression and the local background for all 373 cells found in patients with lung cancer were measured. The local background of each image averaged 375 ± 150 pixel intensity (Supplementary Fig. S2). To account for the localized background effect, the background of each image was subtracted from each measured cell, yielding a corrected PD-L1 pixel intensity range of 17 to 3,090 (Supplementary Fig. S2). We then grouped the cells with the corrected pixel intensities using the SD of background of 0 to 150 pixels as a score of 0 (26% of cells) and twice the SD (151–300 pixels) as a score of 1 (low expression, 42% of cells). For medium expression, a score of 2 (22% of cells) was determined as being twice the mean background signal (301–750 pixel) and high expression or score of 3 (10% of cells) was set at >twice the mean background signal (>750 pixels; Supplementary Fig. S2).

Pixel intensity of PD-L1 in EMTCTCs averaged 384 ± 484 at T0 and 672 ± 669 at T1 ($P = 0.021$), while CAMLs had an average of 182 ± 89 at T0 and 282 ± 169 at T1 ($P = 0.004$; Fig. 5). Regression analysis found a weak, but significant, positive correlation between RAD50 and PD-L1 from T0 to T1 (Pearson $R^2 = 0.079$, $P < 0.0001$, $n = 373$). Although RAD50 was reliably induced from T0 to T1 among patients, changes in PD-L1 expression in individual patients were far more variable (Fig. 5). We found three distinct patterns of PD-L1 expression between T0 and T1 in the 35 patients who were assessable for both time points. Eighteen patients (51%) had no/low PD-L1 expression at both time points, 6 patients (17%) had persistently medium/high PD-L1 at both time points, and 11 patients (32%) saw an increase from a low 0/1 score to a 2/3 score (Fig. 5).

Comparison of PD-L1 levels in the primary tissue, CTCs, and CAMLs

We stained available tissues from the original diagnostic biopsy by IHC using two commercially available and CLIA-certified tests using clones 22c3 and 28-8 (DAKO). Unfortunately, we were only able to retrieve useable tissue or cell blocks from pathologic archives in nine of 41 patients, and one of these nine patients only had sufficient tissue for one IHC test (Fig. 3). This was a result of tumor necrosis or small nodules, resulting in insufficient mass to perform the PD-L1 IHC testing. Of the nine archival samples, only two had positive PD-L1 staining with some variability in the expression scores and percentages between the two tests (Fig. 3C). In comparison, PD-L1 expression was quantifiable in 85% of T0 patient samples ($n = 35/41$) and 100% ($n = 41/41$) in T1 patient samples using the BBB. Specifically at T0, EMTCTCs and CAMLs showed low/negative (score 0/1) PD-L1 expression in 21 patients (60%), medium (score 2) expression in nine patients (26%), and high (score 3) expression in five patients (14%; Fig. 3C).

At T0, expression of PD-L1 in the circulating cells closely paralleled the IHC biopsy results for two IHC-positive stained samples using the 28-8 IHC clone results (Fig. 3C). Three patients had concordant negative PD-L1 tissue by IHC and low (0/1) expression on circulating cells, but three patients had discordant results with negative tissue IHC PD-L1 but 2/3 scores on the circulating cells, and one patient lacked circulating cells in the T0 sample (Fig. 3). Given the limited number of samples, a proper statistical analysis was not possible. However, these results suggest primary biopsies inconsistently provide sufficient tissue for assaying PD-L1 expression, while a BBB approach could measure intrinsic levels and monitor changes of PD-L1 expression in circulating cells originating from cell populations found at the primary lung tumor.

Published OnlineFirst July 5, 2017; DOI: 10.1158/1078-0432.CCR-17-0802

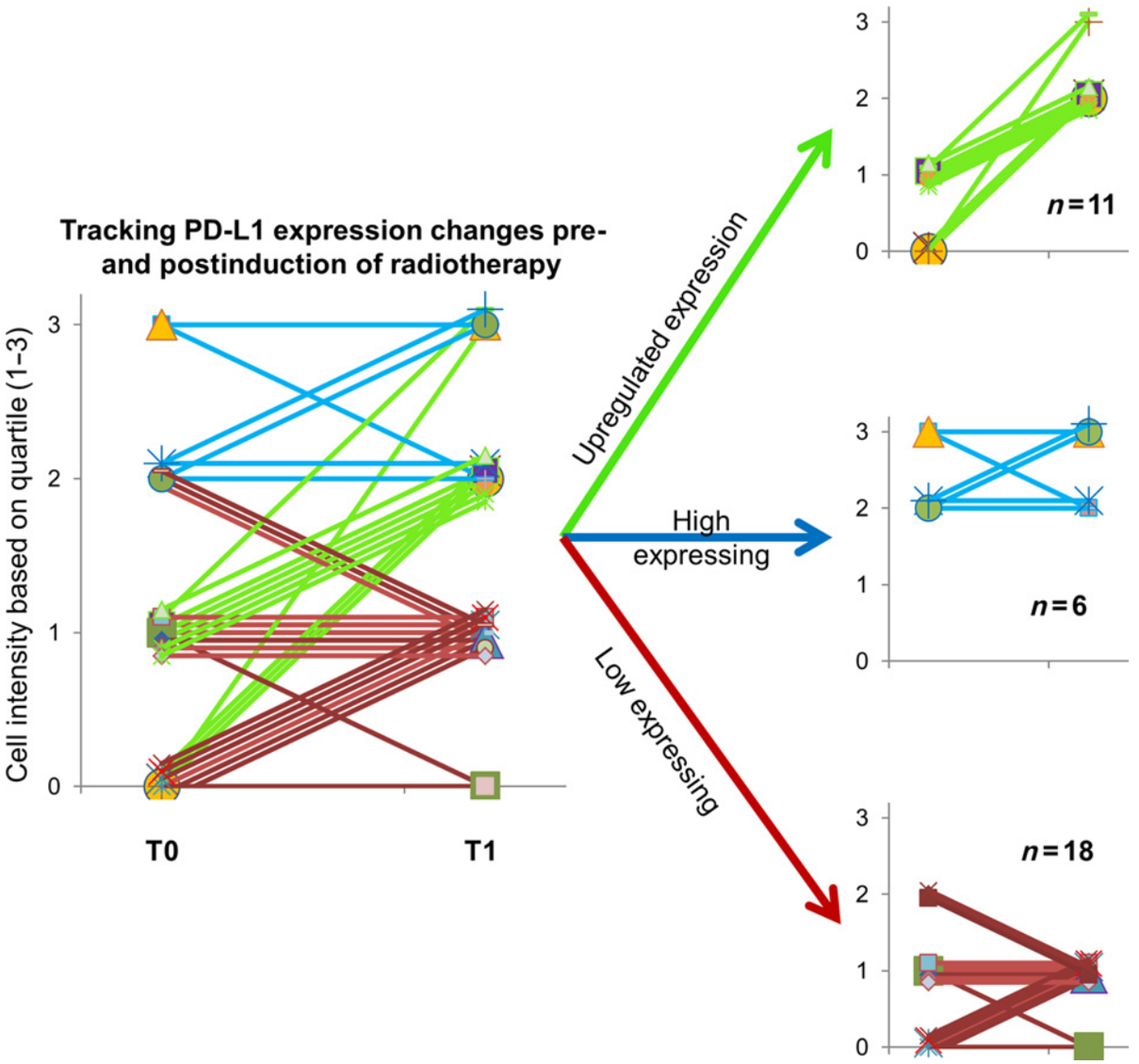

Figure 5.

Scoring and tracking PD-L1 expressions of EMTCTCs and CAMLs in each patient during induction of radiotherapy. The highest expressing cell from each patient was scored 0 to 3 (negative, low, medium, or high). Three distinct patterns emerged, patients with low expressing cells that became high expressing after induction of radiotherapy, patients with consistently high PD-L1–expressing circulating cells, and patients with consistently low expressing circulating cells, $n = 35$ (Supplementary Fig. S6).

PD-L1 and RAD50 in circulating cells as potential prognostic markers

In tissue biopsies, expression of the biomarker PD-L1 alone is not a prognostic indicator of survival in lung cancer, while RAD50 foci formation has been indicated as positively correlated with survival (14, 18, 20, 24, 29, 30, 32, 35, 39, 40, 42). We analyzed the clinical outcomes of patients based on expression of PD-L1, or the average number of RAD50, at both T0 and T1 time points (Fig. 6). For comparing PFS using expression of PD-L1, we used the medium expression as the cut-off criteria, that is, <2 versus ≥2 for the two cohorts. Patients with lower PD-L1 at T0 had a slightly worse HR of 1.8, which was not significant ($P = 0.305$). At T1, patients with lower PD-L1 had a slightly better overall PFS (HR = 0.7), which was also not significant ($P = 0.581$). These data suggest limited to no correlation with overall PFS based on expression of PD-L1 levels at T0 or T1. Using median PFS, we did find a slight trend to better median PFS at T0 in cells with higher PD-L1 (16 months vs. >24 months), but confirmation of this requires a much larger sample size.

Because RAD50 foci formation in tissue biopsies has been shown to be positively correlated with survival (18, 20, 24, 26), we assessed its prognostic value in circulating cells (Fig. 6). The number of RAD50 foci in EMTCTCs and CAMLs at T0 had no clinical difference in overall PFS (HR = 1.0, $P = 0.775$). However, patients with higher RAD50 foci at T1 did nonsignificantly trend to better overall PFS (HR, 2.3; $P = 0.27$; Fig. 6).

Published OnlineFirst July 5, 2017; DOI: 10.1158/1078-0432.CCR-17-0802

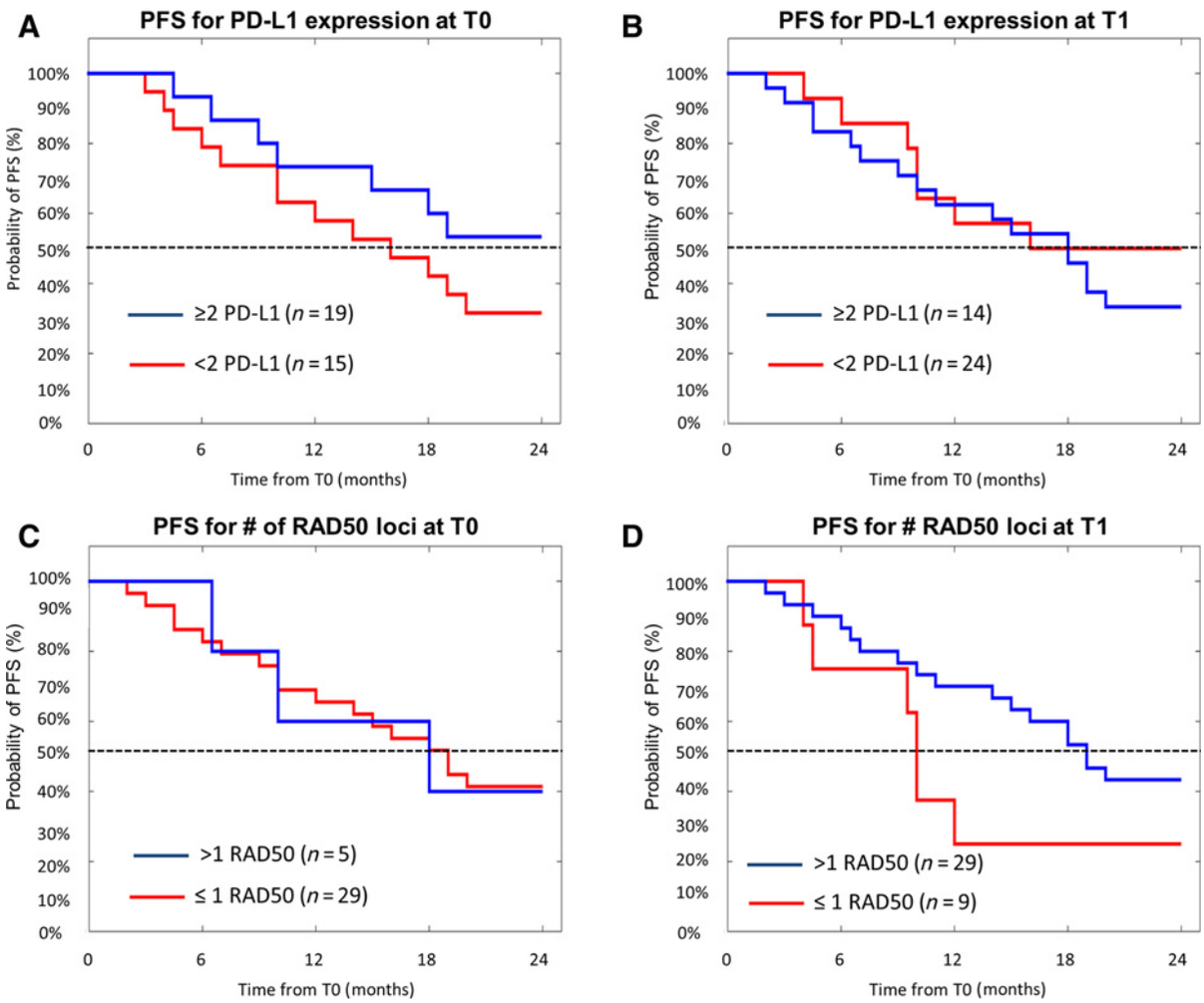

Figure 6.

Comparing the PFS of patients based on high/low PD-L1 expression or RAD50 loci formation pre- and postradiotherapy. **A,** PFS of patients with high PD-L1 expression (2–3 BBB IHC) versus patients with low PD-L1 expression (0–1 BBB IHC) at T0, median PFS 16 versus >24 months. **B,** PFS of patients with high PD-L1 expression versus patients with low PD-L1 expression at T1, median PFS 16 versus 18 months, $P = 0.958$. **C,** PFS of patients averaging $\leq$1 RAD50 loci per circulating cell at T0, median PFS 19 versus 18 months, $P = 0.246$. **D,** PFS of patients averaging $\leq$1 RAD50 loci per circulating cell at T1, median PFS 10 versus 19 months, $P = 0.034$.

Thus, although overall PFS was not significantly different, the median PFS was 1.9× longer in patients with >1 RAD50 foci/cell compared with patients with $\leq$1 RAD50 foci/cell (9.8 months vs. 18.5 months, respectively). These data suggest that a RAD50 increase in circulating cells after radiotherapy may have prognostic value, an observation that will need further validation and larger sample sizes.

Discussion

We prospectively and sequentially tracked PD-L1 levels and RAD50 foci in three circulating blood cell subtypes PDCTCs, EMTCTCs, and CAMLs from 41 patients with lung cancer undergoing (chemo) radiotherapy. We phenotyped circulating cells based on radiation-induced RAD50 foci formation to quantifiably track clear biological changes in cells emanating from a primary lung tumor mass. Furthermore, tracking these dynamic changes might be used to differentiate patients with tumors that may have become more sensitized to radiotherapy, although larger studies are needed.

Many groups have established that the formation of IRIF is observable by RAD50 foci formation in the nuclei of radiation-damaged cells (Supplementary Fig. S4; refs. 18, 20, 23) and inhibition of IRIF formation though prior sensitization with DNA-damaging stressors has been shown to be positively correlated with clinical outcome in a number of cancers (i.e., NSCLC, breast, squamous cell carcinoma, etc.; refs. 18, 20, 23, 24, 26). We initially observed that untreated patients with NSCLC prior to radiotherapy had low numbers of RAD50 foci with a significant rise in RAD50 foci directly in parallel with the induction of radiotherapy. This increase in RAD50 is likely a result of DNA damage caused by the radiotherapeutic

Published OnlineFirst July 5, 2017; DOI: 10.1158/1078-0432.CCR-17-0802

induction, and the RAD50 foci formation in circulating cells appears to act as a noninvasive tracer in cancer patients receiving site-directed radiotherapy. We suggest that RAD50 could be used as in liquid biopsy analyses to confirm the organ of origin of circulating cells and that both EMTCTCs and CAMLs disseminate from primary lung masses in patients.

The currently approved IHC testing of biopsy tissue for PD-L1 expression is only a predictor of response in patients with very high levels of PD-L1 expression, yet many PD-L1–negative patients will also benefit (29, 30, 33, 39–42, 46). This discrepancy may be attributed to the dynamic nature of immune modulation expression and/or the inability to analyze the stromal cell components. Because immune checkpoint protein expression is dynamic, being influenced by multiple microenvironmental, inflammatory, and therapy factors, it has been hypothesized that blood-based analysis may provide a more accurate representation of the current PD-L1 expression in patients (29, 30, 39, 42, 43, 47, 48). Interestingly, we found three classes of PD-L1 responses in the circulating cells of patients, those that are persistently low, persistently high, or inducible from low to high, which occurs in about one-third of patients (32%). This suggests that intrinsically high or inducible PD-L1 levels in nearly half of the patients (49%) could be predictive of immunotherapy response, a hypothesis that will need prospective validation in clinical trials that combine immunotherapy and radiotherapy.

Although there is discordance in the literature regarding expression and prognostic value of PD-L1 in CTCs, our results are more in line with our understanding of PD-L1 expression and prognostic significance in tumor biopsies (24, 47–49). Initial research on PD-L1 in CTCs has given conflicting results based on our understanding of the PD-L1 cascade. In some cases, all patients' CTCs had positive PD-L1 (47); further presence of PD-L1 on CTCs has been identified as a general prognostic indicator of survival (16, 48). These conclusions are in contrast with general IHC testing of primary tumor masses, which finds little to no correlation between PD-L1 expression in biopsies and survival, when PD-L1/PD-1 therapeutics are not used (29–31, 36–41, 46). Furthermore, only a small fraction of patients will actually respond to PD-L1/PD-1 therapy, indicating that the reported CTC assays may be overly sensitive for detecting PD-L1 and will unlikely translate to clinical benefit for PD-L1/PD-1 therapies (16, 47–49). An alternative issue may be that many CTC technologies do not differentiate the EMTCTC subpopulation from the CellSearch CTC population (i.e., PDCTCs), or make any mention of CStCs (3, 4, 6, 7, 16, 17, 47–49). These methods describe a BBB approach that differentiates CAMLs and the PDCTC/EMTCTC subpopulations by well-defined intrinsic biological indicators, that is, EMTCTCs lose EpCAM and downregulate cytokeratin (6, 10, 11, 13, 14, 43). This differentiation appears to allow for more specific analysis, whereby CTCs with separate clinical and biological attributes can be analyzed independently or in conjunction when analyzing clinically relevant biomarkers. Future research may determine whether there is prognostic or predictive value to assessing PD-L1 expression on CTCs or CAMLs.

We hypothesized that sequential tracking of CTCs or circulating immune-stromal cells from the primary lung tumor is feasible using a BBB and potentially can serve as predictive biomarkers for cancer therapies. By differentiating three separate cell types (PDCTCs, EMTCTCs, and CAMLs), we provide a more robust assay for quantifying the dynamics of PD-L1 expression. Although PDCTCs are the subtype of CTCs isolated using the CellSearch platform, it is uncommon in patients with NSCLC and thus of limited value here. EMTCTCs are more prevalent in NSCLC (6–9, 16) with 49% of all our T0 samples containing an EMTCTC, greatly expanding the utility of blood as a surrogate to tissue biopsies in NSCLC. CAMLs were the most prevalent, with 81% of our patients with NSCLC having CAMLs in circulation at baseline and 100% after induction of treatment. Being that both EMTCTCs and CAMLs have been well proven as cancer-specific biomarkers, these data suggest that combining CAMLs and EMTCTCs greatly expands the ability to characterize cellular biomarkers, such as PD-L1, in blood-based diagnosis. Clinically, these results suggest that dynamic biological changes in circulating tumor-derived cells can be quantified in real time and our PD-L1 analyses show that dynamic changes in immune-modulating biomarkers can be consistently tracked in patients with NSCLC, by combining both CTCs and CStCs. Interestingly, sequential analysis of patients 2 to 4 months after completion of therapy ($n = 15$) finds that 87% of the PD-L1 expression remained unchanged from the T1 time point, indicating longevity in PD-L1 expression alterations (Supplementary Table S2). These data suggest that sequentially and noninvasively quantifying PD-L1 expression on multiple cancer-associated cells in circulation appears promising. However, further studies are needed to determine the clinical outcomes or clinical relevance using larger cohorts to evaluate confounding factors such as therapy, disease subtype, and stage. In addition, we must now assess whether PD-L1 on these cell types correlates with clinical benefit of PD-L1/PD-1 therapies and whether tracking and phenotyping circulating cells have stronger predictive utility.

Disclosure of Potential Conflicts of Interest

D.L. Adams and D.K. Adams hold ownership interest (including patents) in Creatv MicroTech, Inc. C.-M. Tang reports receiving commercial research grants from Bria Cell and holds ownership interest (including patents) in Creatv MicroTech, Inc. S.H. Lin reports receiving commercial research grants from Genentech/Roche, Hitachi Chemicals, Peregrine Pharmaceuticals, and STCube Pharmaceuticals and is a consultant/advisory board member for AstraZeneca. No potential conflicts of interest were disclosed by the other authors.

Disclaimer

The content of the information does not necessarily reflect the position or the policy of the U.S. Government.

Authors' Contributions

Conception and design: D.L. Adams, J. He, R. Komaki, Z. Liao, M.J. Edelman, C.-M. Tang, S.H. Lin

Development of methodology: D.L. Adams, J. He, N. Kalhor, S.H. Lin

Acquisition of data (provided animals, acquired and managed patients, provided facilities, etc.): D.L. Adams, J. He, M. Zhang, T. Xu, H. Gao, Y. Qiao, R. Komaki, Z. Liao, M.J. Edelman, S.H. Lin

Analysis and interpretation of data (e.g., statistical analysis, biostatistics, computational analysis): D.L. Adams, D.K. Adams, N. Kalhor, R. Komaki, M.J. Edelman

Writing, review, and/or revision of the manuscript: D.L. Adams, D.K. Adams, T. Xu, J.M. Reuben, R. Komaki, Z. Liao, M.J. Edelman, C.-M. Tang, S.H. Lin

Administrative, technical, or material support (i.e., reporting or organizing data, constructing databases): D.L. Adams, T. Xu, R. Komaki, Z. Liao, C.-M. Tang, S.H. Lin

Study supervision: D.L. Adams, T. Xu, R. Komaki, S.H. Lin

Acknowledgments

We would like to thank all of the patients who contributed to this study.

Grant Support

This work was supported by in part by the Mabuchi Research Fund, the U.S. Army Research Office (ARO), and the Defense Advanced Research Projects Agency (DARPA; W911NF-14-C-0098).

The costs of publication of this article were defrayed in part by the payment of page charges. This article must therefore be hereby marked *advertisement* in accordance with 18 U.S.C. Section 1734 solely to indicate this fact.

Received March 20, 2017; revised May 22, 2017; accepted June 28, 2017; published OnlineFirst July 5, 2017.

References

1. Adams DL, Zhu P, Makarova OV, Martin SS, Charpentier M, Chumsri S, et al. The systematic study of circulating tumor cell isolation using lithographic microfilters. RSC Adv 2014;4:4334–42.
2. Lianidou ES, Markou A. Circulating tumor cells in breast cancer: detection systems, molecular characterization, and future challenges. Clin Chem 2011;57:1242–55.
3. Pantel K, Brakenhoff RH, Brandt B. Detection, clinical relevance and specific biological properties of disseminating tumour cells. Nat Rev Cancer 2008;8:329–40.
4. Paterlini-Brechot P, Benali NL. Circulating tumor cells (CTC) detection: clinical impact and future directions. Cancer Lett 2007;253: 180–204.
5. Adams D, Tsai S, Makarova OV, Zhu P, Li S, Amstutz PT, et al. Low cytokeratin-and low EpCAM-expressing circulating tumor cells in pancreatic cancer. J Clin Oncol 2013;31:11046.
6. Adams DL, Stefansson S, Haudenschild C, Martin SS, Charpentier M, Chumsri S, et al. Cytometric characterization of circulating tumor cells captured by microfiltration and their correlation to the cellsearch((R)) CTC test. Cytometry A 2015;87:137–44.
7. Krebs MG, Hou JM, Sloane R, Lancashire L, Priest L, Nonaka D, et al. Analysis of circulating tumor cells in patients with non-small cell lung cancer using epithelial marker-dependent and -independent approaches. J Thorac Oncol 2012;7:306–15.
8. Farace F, Massard C, Vimond N, Drusch F, Jacques N, Billiot F, et al. A direct comparison of CellSearch and ISET for circulating tumour-cell detection in patients with metastatic carcinomas. Br J Cancer 2011; 105:847–53.
9. Lecharpentier A, Vielh P, Perez-Moreno P, Planchard D, Soria JC, Farace F. Detection of circulating tumour cells with a hybrid (epithelial/mesenchymal) phenotype in patients with metastatic non-small cell lung cancer. Br J Cancer 2011;105:1338–41.
10. Adams DL, Adams DK, Stefansson S, Haudenschild C, Martin SS, Charpentier M, et al. Mitosis in circulating tumor cells stratifies highly aggressive breast carcinomas. Breast Cancer Res 2016;18:44.
11. Adams DL, Adams DK, Alpaugh RK, Cristofanilli M, Martin SS, Chumsri S, et al. Circulating cancer-associated macrophage-like cells differentiate malignant breast cancer and benign breast conditions. Cancer Epidemiol Biomarkers Prev 2016;25:1037–42.
12. Adams DL, Alpaugh RK, Martin SS, Charpentier M, Chumsri S, Cristofanilli M, et al. Precision microfilters as an all in one system for multiplex analysis of circulating tumor cells. RSC Adv 2016;6:6405–14.
13. Adams DL, Alpaugh RK, Tsai S, Tang CM, Stefansson S. Multi-Phenotypic subtyping of circulating tumor cells using sequential fluorescent quenching and restaining. Sci Rep 2016;6:33488.
14. Adams DL, Martin SS, Alpaugh RK, Charpentier M, Tsai S, Bergan RC, et al. Circulating giant macrophages as a potential biomarker of solid tumors. Proc Natl Acad Sci U S A 2014;111:3514–9.
15. Allard WJ, Matera J, Miller MC, Repollet M, Connelly MC, Rao C, et al. Tumor cells circulate in the peripheral blood of all major carcinomas but not in healthy subjects or patients with nonmalignant diseases. Clin Cancer Res 2004;10:6897–904.
16. Anantharaman A, Friedlander T, Lu D, Krupa R, Premasekharan G, Hough J, et al. Programmed death-ligand 1 (PD-L1) characterization of circulating tumor cells (CTCs) in muscle invasive and metastatic bladder cancer patients. BMC Cancer 2016;16:744.
17. Mu Z, Benali-Furet N, Uzan G, Znaty A, Ye Z, Paolillo C, et al. Detection and characterization of circulating tumor associated cells in metastatic breast cancer. Int J Mol Sci 2016;17:pii:E1665.
18. Abuzeid WM, Jiang X, Shi G, Wang H, Paulson D, Araki K, et al. Molecular disruption of RAD50 sensitizes human tumor cells to cisplatin-based chemotherapy. J Clin Invest 2009;119:1974–85.
19. Adams DL, Edelman MJ, Fang P, Jiang W, He J, Xu T, et al. Sequential tracking of PD-L1 expression and RAD50 induction in CTCs and circulating stromal cells of lung cancer patients during treatment with radiotherapy. In: Proceedings of the 107th Annual Meeting of the American Association for Cancer Research; 2016 Apr 16–20; New Orleans, LA. Philadelphia, PA: AACR; 2016.Abstract nr 4990.
20. Flores-Perez A, Rafaelli LE, Ramirez-Torres N, Arechaga-Ocampo E, Frias S, Sanchez S, et al. RAD50 targeting impairs DNA damage response and sensitizes human breast cancer cells to cisplatin therapy. Cancer Biol Ther 2014;15:777–88.
21. Garcia-Villa A, Balasubramanian P, Miller BL, Lustberg MB, Ramaswamy B, Chalmers JJ. Assessment of gamma-H2AX levels in circulating tumor cells from patients receiving chemotherapy. Front Oncol 2012;2:128.
22. Lin SH, He J, Edelman M, Xu T, Gao H, Reuben J, et al. Sequential assessment of DNA damage response and PD-L1 expression in circulating tumor cells of lung cancer patients during radiotherapy. J Thorac Oncol 2015;10:S266–S267.
23. Maser RS, Monsen KJ, Nelms BE, Petrini JH. hMre11 and hRad50 nuclear foci are induced during the normal cellular response to DNA double-strand breaks. Mol Cell Biol 1997;17:6087–96.
24. Wang LH, Pfister TD, Parchment RE, Kummar S, Rubinstein L, Evrard YA, et al. Monitoring drug-induced gammaH2AX as a pharmacodynamic biomarker in individual circulating tumor cells. Clin Cancer Res 2010;16:1073–84.
25. Gatei M, Jakob B, Chen P, Kijas AW, Becherel OJ, Gueven N, et al. ATM protein-dependent phosphorylation of Rad50 protein regulates DNA repair and cell cycle control. J Biol Chem 2011;286:31542–56.
26. Teng SC, Wu KJ, Tseng SF, Wong CW, Kao L. Importin KPNA2, NBS1, DNA repair and tumorigenesis. J Mol Histol 2006;37:293–9.
27. Demaria S, Golden EB, Formenti SC. Role of local radiation therapy in cancer immunotherapy. JAMA Oncol 2015;1:1325–32.
28. Derer A, Deloch L, Rubner Y, Fietkau R, Frey B, Gaipl US. Radio-immunotherapy-induced immunogenic cancer cells as basis for induction of systemic anti-tumor immune responses - pre-clinical evidence and ongoing clinical applications. Front Immunol 2015;6:505.
29. Brahmer J, Reckamp KL, Baas P, Crino L, Eberhardt WE, Poddubskaya E, et al. Nivolumab versus docetaxel in advanced squamous-cell non-small-cell lung cancer. N Engl J Med 2015;373:123–35.
30. Brahmer JR, Tykodi SS, Chow LQ, Hwu WJ, Topalian SL, Hwu P, et al. Safety and activity of anti-PD-L1 antibody in patients with advanced cancer. N Engl J Med 2012;366:2455–65.
31. Garon EB, Rizvi NA, Hui R, Leighl N, Balmanoukian AS, Eder JP, et al. Pembrolizumab for the treatment of non-small-cell lung cancer. N Engl J Med 2015;372:2018–28.
32. Gettinger SN, Horn L, Gandhi L, Spigel DR, Antonia SJ, Rizvi NA, et al. Overall survival and long-term safety of nivolumab (anti-programmed death 1 antibody, BMS-936558, ONO-4538) in patients with previously treated advanced non-small-cell lung cancer. J Clin Oncol 2015;33:2004–12.
33. Ilie M, Long-Mira E, Bence C, Butori C, Lassalle S, Bouhlel L, et al. Comparative study of the PD-L1 status between surgically resected specimens and matched biopsies of NSCLC patients reveal major discordances: a potential issue for anti-PD-L1 therapeutic strategies. Ann Oncol 2016;27:147–53.

Published OnlineFirst July 5, 2017; DOI: 10.1158/1078-0432.CCR-17-0802

34. Reck M, Rodriguez-Abreu D, Robinson AG, Hui R, Csoszi T, Fulop A, et al. Pembrolizumab versus chemotherapy for PD-L1-positive non-small-cell lung cancer. N Engl J Med 2016;375:1823–33.
35. Sundar R, Cho BC, Brahmer JR, Soo RA. Nivolumab in NSCLC: latest evidence and clinical potential. Ther Adv Med Oncol 2015;7: 85–96.
36. Topalian SL, Hodi FS, Brahmer JR, Gettinger SN, Smith DC, McDermott DF, et al. Safety, activity, and immune correlates of anti-PD-1 antibody in cancer. N Engl J Med 2012;366:2443–54.
37. Antonia S, Goldberg SB, Balmanoukian A, Chaft JE, Sanborn RE, Gupta A, et al. Safety and antitumour activity of durvalumab plus tremelimumab in non-small cell lung cancer: a multicentre, phase 1b study. Lancet Oncol 2016;17:299–308.
38. Borghaei H, Paz-Ares L, Horn L, Spigel DR, Steins M, Ready NE, et al. Nivolumab versus docetaxel in advanced nonsquamous non-small-cell lung cancer. N Engl J Med 2015;373:1627–39.
39. Ma W, Gilligan BM, Yuan J, Li T. Current status and perspectives in translational biomarker research for PD-1/PD-L1 immune checkpoint blockade therapy. J Hematol Oncol 2016;9:47.
40. Taube JM, Klein A, Brahmer JR, Xu H, Pan X, Kim JH, et al. Association of PD-1, PD-1 ligands, and other features of the tumor immune microenvironment with response to anti-PD-1 therapy. Clin Cancer Res 2014;20: 5064–74.
41. Herbst RS, Soria JC, Kowanetz M, Fine GD, Hamid O, Gordon MS, et al. Predictive correlates of response to the anti-PD-L1 antibody MPDL3280A in cancer patients. Nature 2014;515:563–7.
42. Ung C, Kockx MM. Challenges & perspectives of immunotherapy biomarkers & the HistoOncoImmune™ methodology. Expert Rev Precision Med Drug Dev 2016;1:9–24.
43. Zhu P, Stanton ML, Castle EP, Joseph RW, Adams DL, Li S, et al. Detection of tumor-associated cells in cryopreserved peripheral blood mononuclear cell samples for retrospective analysis. J Transl Med 2016;14:198.
44. Alix-Panabieres C, Pantel K. Challenges in circulating tumour cell research. Nat Rev Cancer 2014;14:623–31.
45. Marrinucci D, Bethel K, Kolatkar A, Luttgen MS, Malchiodi M, Baehring F, et al. Fluid biopsy in patients with metastatic prostate, pancreatic and breast cancers. Phys Biol 2012;9:016003.
46. Callahan MK, Ott PA, Odunsi K, Bertolini SV, Pan LS, Venhaus RR, et al. A phase 1 study to evaluate the safety and tolerability of MEDI4736, an anti-PD-L1 antibody, in combination with tremelimumab in patients with advanced solid tumors. J Clin Oncol 2014;32:(15 suppl) TPS3120.
47. Mazel M, Jacot W, Pantel K, Bartkowiak K, Topart D, Cayrefourcq L, et al. Frequent expression of PD-L1 on circulating breast cancer cells. Mol Oncol 2015;9:1773–82.
48. Satelli A, Batth IS, Brownlee Z, Rojas C, Meng QH, Kopetz S, et al. Potential role of nuclear PD-L1 expression in cell-surface vimentin positive circulating tumor cells as a prognostic marker in cancer patients. Sci Rep 2016;6:28910.
49. Nicolazzo C, Raimondi C, Mancini M, Caponnetto S, Gradilone A, Gandini O, et al. Monitoring PD-L1 positive circulating tumor cells in non-small cell lung cancer patients treated with the PD-1 inhibitor Nivolumab. Sci Rep 2016;6:31726.

Published OnlineFirst July 5, 2017; DOI: 10.1158/1078-0432.CCR-17-0802

Clinical Cancer Research

Sequential Tracking of PD-L1 Expression and RAD50 Induction in Circulating Tumor and Stromal Cells of Lung Cancer Patients Undergoing Radiotherapy

Daniel L. Adams, Diane K. Adams, Jianzhong He, et al.

Clin Cancer Res 2017;23:5948-5958. Published OnlineFirst July 5, 2017.